Available online at www.sciencedirect.com

ScienceDirect

Procedia CIRP 92 (2020) 163–168

www.elsevier.com/locate/procedia

16th CIRP Conference on Computer Aided Tolerancing (CIRP CAT 2020)

Robustness of geometric verification by segmentation-free X-ray computed tomography

Stefano Petrò[a,*], Giovanni Moroni[a]

[a]*Department of Mechanical Engineering, Politecnico di Milano, Via Giuseppe La Masa, 20156 Milano, Italy*

Abstract

Additive manufacturing technologies can benefit from the use of volumetric representations at design, manufacture, and verification level. Concerning geometric verification, a method has been proposed for testing the conformance to a "volumetric tolerance" specification using X-ray computed tomography (XCT). The method does not require the segmentation of the XCT image, a significant contributor to the measurement uncertainty. This work revises the method, and experimentally investigates its robustness when the XCT scan parameters are varied in the range that guarantees good quality images. The method is proved robust but is also found influenced by the voxel size (image resolution).

Keywords: X-ray computed tomography; Geometric inspection; Segmentation; Enriched Voxel-based representation; Complex geometries; Robustness.

1. Introduction

The design [19], production [1, 17], and verification [9] of additive manufacturing products can still improve significantly. Really taking advantage of additive manufacturing requires that new methodologies for these activities are developed. As "design for" rules are defined for every manufacturing technology, additive manufacturing needs as well his own rules. In the opinion of the authors, this will require a shift from a surface representation of parts to a volumetric representation. This is coherent with the additive manufacturing paradigm: filling a volume rather than generating a surface. Software able to drive additive manufacturing systems without the need of a .stl representation are already available [21]. Volumetric representations of parts are coherent with the application of topological optimization [15], too. Topological optimization of structures tries to define the minimum quantity of material required to still guarantee their compliance. This is done by simulating the addition or removal of material in a volume. Finally, volumetric representations are flexible in the representation of complex geometries.

The authors of this paper have proposed the use of an "enriched voxel based volumetric representation" [14] to completely describe additive manufacturing parts. The base idea is to add "layers" of information to each single voxel, enabling a local specification of the part properties. This may include, but is not limited to, information about material, involvement in mating surfaces, deposition layer. Of course, a similar representation needs to be specified in a proper file format. Fuji Xerox Co., Ltd [18] is developing a similar language.

An enriched voxel based volumetric representation can express geometric tolerances coherently with topological optimization. Topological optimization should return a "minimum material continuum" (the material that must be present to guarantee the structural integrity of the part) and a "maximum material continuum" (the volume of material that can be filled without affecting the part functionality, lightweightness, and cost). These continua define a limit to the geometric variation of the part. Membership to either continuum can be easily specified volumetrically.

Of course, this volumetric geometric tolerance needs to be verified. X-ray computed tomography (XCT) [2, 4, 8] is becoming the most adopted technology to verify additive manufacturing (AM) parts. Differing from conventional coordinate metrology, XCT is not affected by accessibility (contact coordinate measuring systems) or visibility (non-contact systems) issues. In addition, XCT generates a volumetric representation of the X-ray attenuation inside parts. This allows the study of porosity, inclusions, voids and all internal defects which are found in AM parts. XCT can also inspect part geometry, and

* Corresponding author. Tel.: +39 02 2399 8530.
E-mail address: stefano.petro@polimi.it (Stefano Petrò).

10.1016/j.procir.2020.05.184

in particular complex and internal geometries typical of AM parts. The common practice in using XCT to verify parts requires the XCT image is segmented (meshed) and compared to the nominal geometry. However, segmentation has been found to be among the most relevant contributions to the measurement uncertainty [13]. But the output of an XCT scan is a volumetric representation of the part: why not comparing directly the XCT image to the voxel representation of the part? This possibility of a volumetric verification of geometric tolerances has already been envisaged and a methodology has been proposed, but still needs to be completely developed [12].

This paper has two aims. The first one is to introduce a case study and fully develop the proposed methodology for it in order to make it clearer. This has not been done in any previous paper [12, 14]. The second aim is to investigate the robustness of the methodology. When an XCT scan is performed a series of parameters have to be selected by the operator. With different choices of the parameters reasonable quality XCT images can be obtained which are adequate for non-destructive inspection, but insufficient for segmentation and geometric verification. If the proposed methodology is robust against scan parameter setting, this would be another advantage compared to the segmentation-based approach. The case study in §2 is used for an experiment in which the XCT scan parameters are varied, and the the variation effect is studied on the "mutual information" on which the volumetric verification is based. The interpretation of the results will prove the methodology robustness.

2. Case study and procedure for volumetric verification

The data to be analyzed is a series of mutual information values obtained in different XCT scan conditions. In this section the case study is introduced and it is explained how the data is handled to obtain the mutual information values.

The considered case study is a small (about 20 mm high) puppet made by selective laser melting of stainless steel powder (Fig. 1). The model of the puppet, in .stl format (Fig. 2), is freely accessible on cults3d.com [5]. Only the head of the puppet is considered. The reasons behind this choice are as follows. First, the head of the puppet has an approximately spherical geometry, and this makes easier to handle both manual and automatic alignment. Furthermore, the approximately spherical geometry makes easier to understand geometric errors like shape or size deviations. Finally, the part is constituted only by a limited number of triangles, which are of course nominally planar. If, in the future, one would consider the nominal planar geometry of the triangles, this would be possible.

The .stl representation of the puppet has been converted in a voxel representation using the Matlab™ "inpolyhedron" function [6]. This function simply converts a mesh into a grid of values $nv_{i,j,k}$. Each value of the the grid corresponds to a voxel, whose size has been chosen identical to the voxel size in the XCT image. The $nv_{i,j,k}$ value is set as:

$$nv_{i,j,k} = \begin{cases} 0, \text{ the voxel is inside the mesh} \\ 1, \text{ the voxel is outside the mesh} \end{cases} \quad (1)$$

Fig. 1. Picture of the selected case study.

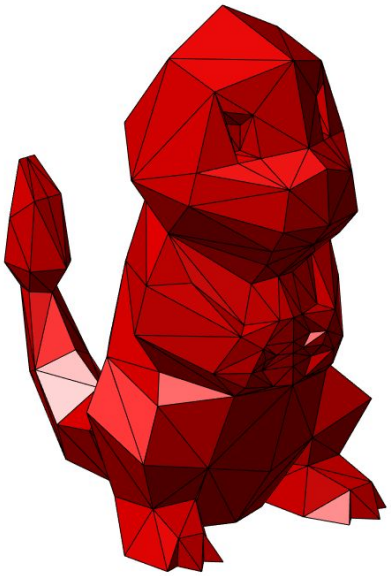

Fig. 2. STL model of the selected case study.

The result of the application of (1) is shown in Fig. 3 (left).

The puppet was scanned on an NSI X25 XCT scanner. The scan parameters are reported in §3, as they are parameters of the experiment and change in each scan. A typical XCT image of the puppet head in shown in Fig. 3 (right). In this measured voxel representation of the puppet head the "gray value" $mv_{i,j,k}$ of each voxel is proportional to the X-ray attenuation at location i, j, k.

In order to allow the comparison of the nominal and measured voxel representations of the puppet head, the two must be registered, so that they occupy (approximately) the same portion of space. The nominal and measured representations are heterogeneous in nature: the nominal representation is, according to (1), binary, while in the measured representation there

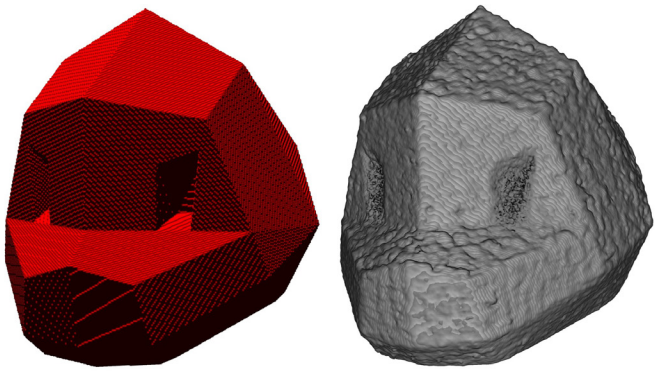

Fig. 3. Voxel representation of the case study. On the left: nominal geometry; on the right: XCT image.

is a full range of $mv_{i,j,k}$. When heterogeneous representations are involved, the literature [16] suggests the mutual information [3] as maximization parameter for the registration instead of the correlation, adopted when the representation are homogeneous. Mutual information is usually defined, in information theory, as the "amount of information shared by two signals". The amount of information of voxel representation defined by the gray values $v_{i,j,k}$ can be measured by the Shannon's entropy:

$$H(A) = -\sum_{o=1}^{n_{GV}} \frac{n_o}{n_{vox}} \log_2 \frac{n_o}{n_{vox}} \tag{2}$$

where n_{vox} is the total number of voxels, n_{GV} is the number of possible values a voxel can assume (e.g. in a 8-bit XCT image $n_{GV} = 256$, or in nominal voxel representation $n_{GV} = 2$), and n_o is the number of occurrences of the o^{th} possible gray value. If a couple of voxel representations (e.g. nominal and measured) is considered, its joint entropy $H(A, B)$ can be similarly defined, simply considering (instead of n_o) $n_{o,r}$ as the number occurrences of the couple constituted by the o^{th} possible gray value in some voxel in the first representation and the r^{th} in the corresponding voxel of the second representation; of course, n_{GV} is now the number of possible combinations of values. The joint entropy measures the total information in the two representations. Finally, the mutual information of two volumetric representations is defined as

$$I(A, B) = H(A) + H(B) - H(A, B) \tag{3}$$

In a previous paper [14] it has been shown that the maximization of the mutual information is an effective criterion for the registration of a nominal and a measured voxel representation of a part. Fig. 4 shows the difference between the nominal and measured voxel representations after the registration. The fuchsia portion of the image is from the measured representation, while the blue one is from the nominal. As expected the

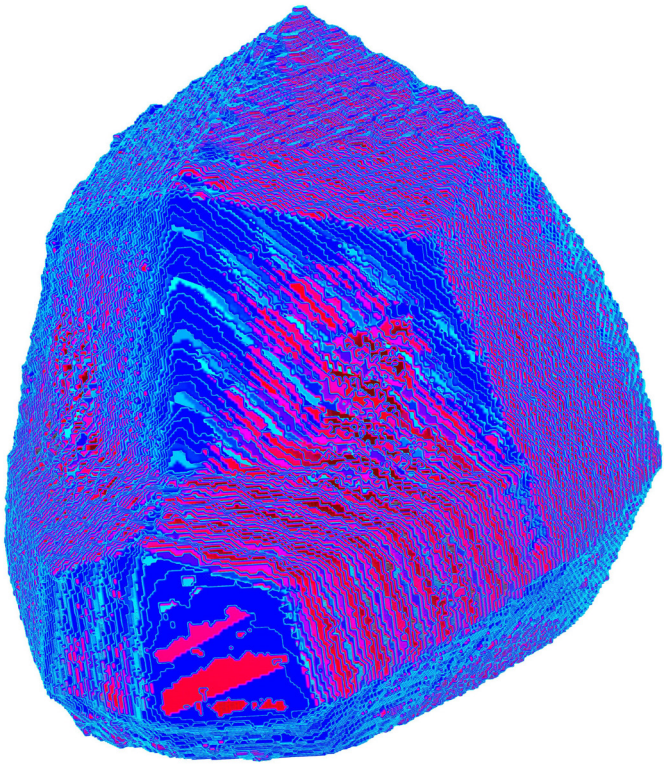

Fig. 4. Registration of the nominal and measured voxel representations.

overlap is not complete, as the part, and hence its measured representation differs from the nominal geometry.

Now, define the volumetric geometric tolerance. The voxels that must be filled by material to guarantee the part functionality are "inside the minimum material continuum" and are characterized by the value 2. The voxels that must be empty are "outside the maximum material continuum" and are set equal to 0. The remaining portion of volume between the two is the "transition zone". A simple way of defining a volumetric tolerance on the part is to define all the voxels "on the boundary" of the nominal representation as belonging to the transition zone. Consider the neighborhood of a voxel, that is $N\left\{v_{i,j,k}\right\} = \bigcup_{o,p,q\in\{-1,0,1\}} v_{o+i,p+j,q+k} - v_{i,j,k}$. The toleranced volumetric representation in this case is

$$tv_{i,j,k} = \begin{cases} 0, \ \forall nv_{o,p,q} \in \left\{N\left\{nv_{i,j,k}\right\} \cup nv_{i,j,k}\right\} | nv_{o,p,q} = 0 \\ 1, \ \begin{array}{l}\left\{\exists nv_{o,p,q} \in \left\{N\left\{nv_{i,j,k}\right\} \cup nv_{i,j,k}\right\} | nv_{o,p,q} = 0\right\} \wedge \\ \wedge \left\{\exists nv_{o,p,q} \in \left\{N\left\{nv_{i,j,k}\right\} \cup nv_{i,j,k}\right\} | nv_{o,p,q} = 1\right\}\end{array} \\ 2, \ \forall nv_{o,p,q} \in \left\{N\left\{nv_{i,j,k}\right\} \cup nv_{i,j,k}\right\} | nv_{o,p,q} = 1 \end{cases} \tag{4}$$

This way a tolerance zone characterized by a width approximately equal to twice the voxel width is obtained. Additional "layers" of voxels can be similarly added to yield a thicker tolerance zone. Fig. 5 shows an example of tolerance zone generated this way.

A criterion has been proposed in a previous paper [12] to verify whether the part conforms to the tolerance or not. The

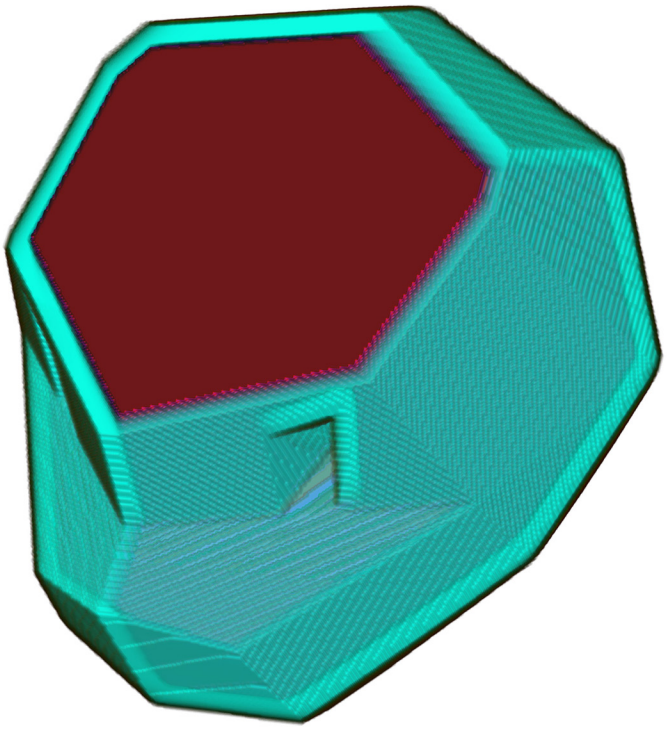

Fig. 5. Example of transition zone (turquoise area).

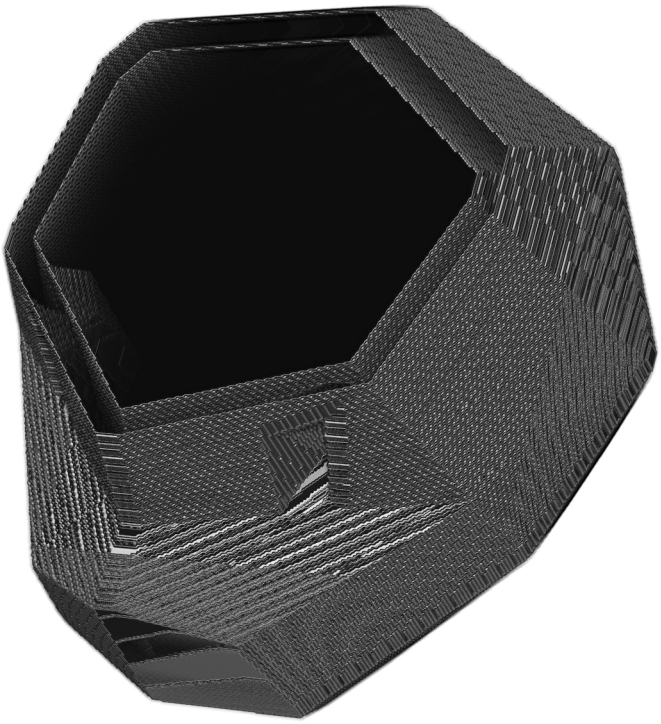

Fig. 6. Example of shells related to the volumetric tolerance representation in Fig. 5.

criterion is based again on the mutual information. In particular, it considers the "inner" and the "outer" neighboring shells. Shells include the voxels out of the tolerance zone, but directly adjacent to it. Mathematically, they can be defined as

$$sv_{i,j,k} = \begin{cases} 0, \left\{ \nexists tv_{o,p,q} \in N\left\{tv_{i,j,k}\right\} | tv_{o,p,q} = 1 \right\} \wedge tv_{i,j,k} = 0 \\ 1, tv_{o,p,q} = 1 \\ 2, \left\{ \nexists tv_{o,p,q} \in N\left\{tv_{i,j,k}\right\} | tv_{o,p,q} = 1 \right\} \wedge tv_{i,j,k} = 2 \\ 3, \left\{ \exists tv_{o,p,q} \in N\left\{tv_{i,j,k}\right\} | tv_{o,p,q} = 1 \right\} \wedge tv_{i,j,k} = 2 \\ 4, \left\{ \exists tv_{o,p,q} \in N\left\{tv_{i,j,k}\right\} | tv_{o,p,q} = 1 \right\} \wedge tv_{i,j,k} = 0 \end{cases} \quad (5)$$

Voxels equal to 3 belong to the inner shell, and voxels equal to 4 belong to the outer shell. An example of shells is shown in Fig. 6.

Now, if the shells only are considered as a single signal (sorted sequence of values), the only relevant information that can be found in their nominal representation is that "they are completely separated", i.e. they do not share any value. The mutual information measures the information shared by two signals. If the mutual information $I(NSN, NSM)$ of the nominal neighboring shells (NSN) and the measured neighboring shells (NSM) is equal to the entropy of NSN, the NSM contain all the information in NSN. But this means that the NSM contain the "complete separation" information: the tolerance is verified. Mathematically, this corresponds to the condition:

$$NMI(NSN, NSM) = \frac{I(NSN, NSM)}{\min\{H(NSN), H(NSM)\}} = 1 \quad (6)$$

NMI is called "normalized mutual information" [20]. The shells are the first portion of the volume affected by a geometric deviation, so any significant geometric or size deviation should alter them and generate a "non-conforming" result. Furthermore, neglecting any other portion of the volume avoids defects like porosity or XCT artifacts affect the verification result.

3. Design and analysis of experiments

The aim of this work is to test whether the procedure described in §2 is robust to an incorrect definition of the XCT scan parameters. In general, if the parameters are not correctly set, XCT artifacts, e.g. beam hardening, can be generated, which affect the image quality. An experiment has been conducted to verify this.

A series of 13 XCT scan have been run on an NSI X25 XCT scanner. The experiment was planned as a 2^3 factorial experiment [11] with no replica, plus a center point replicated five times. The center point parameter set is chosen in the middle of the corner points. The X-ray source voltage, detector integration time, and the number of projections were selected as factors for the experiment. X-ray source intensity was not considered as factor. Fixing simultaneously voltage, integration time, and intensity can lead to low quality XCT images. As such, intensity was set in every combination of voltage and integration time to yield good quality images. A 2.5 mm steel filter was always present during the scans to reduce the beam hardening. The levels of the factors are reported in Tab. 1. These levels where chosen as "reasonable". These are all values an operator

Table 1. Levels of the factors considered in the experiment for the XCT scans.

	Level		
Factor	**Low**	**Center**	**High**
Voltage [KV]	120	140	160
Integration time [fps]	6.62	13.24	24.47
Number of projections	300	600	900

could choose to perform the scan, and in fact all the acquired images where adequately good. However, they were different in terms of contrast, residual artifacts, etc.

Each scan was then reconstructed to obtain a 16bit measured volumetric representation $mv_{i,j,k}$. The original voxel size yielded was equal to 17.67 µm, and each scan had an image size equal to 501x466x540 voxels. To allow the evaluation of the effect of the image resolution, a new series of measured volumetric representations was generated by re-sampling to a voxel size equal to 35.34 µm (image size equal to 250x233x270 voxels). The transition zone was set to have a width approximately equal to 70.68 µm in all cases (two voxels for the low resolution images, four voxels for the high resolution images). The final results are then constituted by 23 evaluations of the mutual information and normalized mutual information.

The evaluated mutual information values where the subject of an analysis of variance. The model hypotheses (normality, homoscedasticity, independence) were verified. The results of the analysis are summarized in Fig. 7: it is apparent that the voxel size generates a more relevant effect than the other factors. From a statistical point of view, only the voxel size is significant, as indicated in Tab. 2: the variation induced by the parameters setting is not distinguishable from the natural variability of the mutual information due to scan repetitions. This proofs the robustness of the procedure proposed in §2 when the parameters of the XCT scan are set in a reasonable range. The effect of the variation of voxel size indicates instead that the resolution may affect the volumetric geometric tolerance verification. Fig. 7 shows that when the voxels are larger, the mutual information is larger. This may be explained by the fact that the higher the resolution the larger the information contained in NSM. This makes the test more sensitive to any deviation of geometry or size, and then the mutual information values smaller. This is similar to saying that the higher resolution makes the non-conformance statement less uncertain. Finally, the standard deviation of the pure error, which is an estimate of the natural variability of the mutual information, is equal to 0.074.

If the normalized mutual information is analyzed instead of the mutual information the results are (almost) identical (Fig. 8). This might be expected. Since the NSN contains only two possible values, while the NSM contains a 16bit signal, $H(NSN) < H(NSM)$. Hence the denominator in (6) is always equal to $H(NSN)$. But $H(NSN)$ does not depend on the scan parameters, so their effect must be the same either considering $I(NSN, NSM)$ or $NMI(NSN, NSM)$. Furthermore, it is easy to show that in the considered case $H(NSN)$ is slightly affected by the resolution. In fact, if the transition zone is defined according to (4), regardless of the resolution the number of voxels in the inner shell will be almost identical to the number of

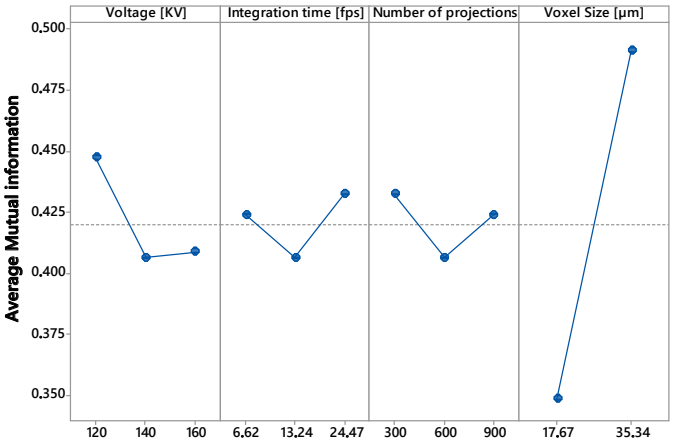

Fig. 7. Mutual information main effect plot for voltage, integration time, number of projections, and voxel size versus the mutual information.

Table 2. ANOVA table (up to the second order interactions).

Term	**Coef**	**SE Coef**	**P-Value**
Constant	0,4283	0,0178	0,000
Voltage	-0,0193	0,0178	0,297
Integration time	0,0042	0,0178	0,816
Number of projections	-0,0042	0,0178	0,817
Voxel Size	0,0740	0,0141	0,000
*Voltage*Integration time*	-0,0339	0,0178	0,078
*Voltage*Number of projections*	0,0095	0,0178	0,604
*Voltage*Voxel Size*	0,0086	0,0178	0,638
*Integration time*Number of projections*	-0,0010	0,0178	0,958
*Integration time*Voxel Size*	0,0274	0,0176	0,142
*Number of projections*Voxel Size*	-0,0078	0,0178	0,667

voxels in the outer shell. Applying (2) to calculate $H(NSN)$ to them yields approximately the same value, and in particular a value close to 1: the actual value of $H(NSN)$ when the voxel size is equal to 35.34 µm is 0.9970, and it is 0.9992 when the voxel size is equal to 17.67 µm. This justifies the fact that Fig. 7 and Fig. 8 are visually identical. Hence the results for the analysis of variance of the normalized mutual information are (almost) equal to the result obtained for the mutual information and are not reported.

4. Conclusions

In the opinion of the authors, a transition will happen for additive manufacturing from conventional to volumetric representation of parts. This to guarantee higher flexibility and compatibility with the technologies involved (topological optimization, additive manufacturing itself, and XCT). But new tools are needed to allow this transition.

A new study on the method for the volumetric verification of geometric tolerances of additive manufacturing parts has been proposed. It has been shown that the proposed methodology is

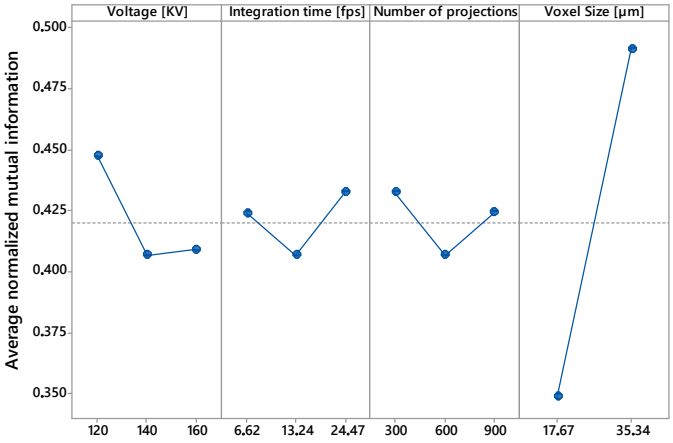

Fig. 8. Normalized Mutual information main effect plot for voltage, integration time, number of projections, and voxel size versus the mutual information.

robust to the variation of XCT scan parameters. This makes the proposed methodology applicable with confidence.

The study has shown also that the proposed methodology is sensitive to the XCT image voxel size. This is due to the increased amount of information that can be found in high resolution images, which alter the value of the mutual information the volumetric verification is based on.

The next steps of the research on the volumetric verification of geometric tolerances include, first of all, a quantification of the reliability of the method in terms of probability of inspection errors [7]. This actually also extends the proposed results to any other condition. Then, to consider the identified impact of the voxel size, the possibility of using XCT image analysis for the improvement of image resolution will be studied. Finally, the adoption of more advanced representation like Octree [10], capable of handling higher resolution without an excessive data accumulation, will be considered.

Acknowledgements

Financial support to this work has been provided as part of the project AMALA – Advanced Manufacturing Laboratory, funded by Politecnico di Milano (Italy), CUP: D46D13000540005.

The authors wish to thank Trumpf GMbH for providing the TruPrint 3000 system on which the case study was printed, and Ms. Valentina Finazzi for her support in the printing process.

References

[1] Bourell, D., Kruth, J.P., Leu, M., Levy, G., Rosen, D., Beese, A.M., Clare, A., 2017. Materials for additive manufacturing. CIRP Annals - Manufacturing Technology 66, 659–681. doi:10.1016/j.cirp.2017.05.009.

[2] Carmignato, S., Dewulf, W., Leach, R., 2017. Industrial X-ray computed tomography. 1 ed., Springer International Publishing, Cham, Switzerland. doi:10.1007/978-3-319-59573-3.

[3] Cover, T.M., Thomas, J.A., 2005. Entropy, Relative Entropy, and Mutual Information, in: Elements of Information Theory. 2 ed.. Wiley. chapter 2, pp. 13–55. doi:10.1002/047174882X.ch2.

[4] De Chiffre, L., Carmignato, S., Kruth, J.P., Schmitt, R., Weckenmann, A., 2014. Industrial applications of computed tomography. CIRP Annals - Manufacturing Technology 63, 655–677. doi:10.1016/j.cirp.2014.05.011.

[5] Flowalistik, A., 2020. Low-Poly Charmander.

[6] Holcomb, S., 2012. inpolyhedron - are points inside a triangulated volume? URL: https://it.mathworks.com/matlabcentral/fileexchange/37856-inpolyhedron-are-points-inside-a-triangulated-volume.

[7] Joint Committee for Guides in Metrology, 2012. ISO/IEC GUIDE 98-4: Uncertainty of measurement - Part 4: Role of measurement uncertainty in conformity assessment.

[8] Kruth, J.P., Bartscher, M., Carmignato, S., Schmitt, R., De Chiffre, L., Weckenmann, A., 2011. Computed tomography for dimensional metrology. CIRP Annals - Manufacturing Technology 60, 821–842. doi:10.1016/j.cirp.2011.05.006.

[9] Leach, R.K., Bourell, D., Carmignato, S., Donmez, A., Senin, N., Dewulf, W., 2019. Geometrical metrology for metal additive manufacturing. CIRP Annals - Manufacturing Technology 68, 677–700. doi:10.1016/j.cirp.2019.05.004.

[10] Meagher, D., 1980. Octree Encoding: A New Technique for the Representation, Manipulation and Display of Arbitrary 3-D Objects by Computer. Technical Report IPL-TR-80-111. Rensselaer Polytechnic Institute.

[11] Montgomery, D.C., 2017. Design and Analysis of Experiments. 9 ed., John Wiley & Sons, Inc., Hoboken, NJ.

[12] Moroni, G., Petrò, S., 2018. Segmentation-free geometrical verification of additively manufactured components by x-ray computed tomography. CIRP Annals - Manufacturing Technology 67, 519–522. doi:10.1016/j.cirp.2018.04.011.

[13] Moroni, G., Petrò, S., 2019. An experimental study on segmentation in X-Ray Computed Tomography, in: The E-Journal Of nondestructive Testing, pp. 1–7. URL: http://www.ndt.net/?id=23731.

[14] Moroni, G., Petrò, S., Polini, W., 2017. Geometrical product specification and verification in additive manufacturing. CIRP Annals - Manufacturing Technology 66, 157–160. doi:10.1016/j.cirp.2017.04.043.

[15] Plocher, J., Panesar, A., 2019. Review on design and structural optimisation in additive manufacturing: Towards next-generation lightweight structures. Materials and Design 183, 108164. doi:10.1016/j.matdes.2019.108164.

[16] Pluim, J., Maintz, J., Viergever, M., 2003. Mutual-information-based registration of medical images: a survey. IEEE Transactions on Medical Imaging 22, 986–1004. doi:10.1109/TMI.2003.815867.

[17] Schmidt, M., Merklein, M., Bourell, D., Dimitrov, D., Hausotte, T., Wegener, K., Overmeyer, L., Vollertsen, F., Levy, G.N., 2017. Laser based additive manufacturing in industry and academia. CIRP Annals - Manufacturing Technology 66, 561–583. doi:10.1016/j.cirp.2017.05.011.

[18] Takahashi, T., Masumori, A., Fujii, M., Tanaka, H., 2018. FAV (Fabricatable Voxel) File Format Specification. URL: https://www.fujixerox.com/eng/company/technology/communication/3d/fav.html.

[19] Thompson, M.K., Moroni, G., Vaneker, T., Fadel, G., Campbell, R.I., Gibson, I., Bernard, A., Schulz, J., Graf, P., Ahuja, B., Martina, F., 2016. Design for Additive Manufacturing: Trends, opportunities, considerations, and constraints. CIRP Annals - Manufacturing Technology 65, 737–760. doi:10.1016/j.cirp.2016.05.004.

[20] Yao, Y.Y., 2003. Information-Theoretic Measures for Knowledge Discovery and Data Mining. Springer Berlin Heidelberg, Berlin, Germany. volume 119 of *Studies in Fuzziness and Soft Computing*. chapter 6. pp. 115–136. doi:10.1007/978-3-540-36212-8_6.

[21] ZMorph, 2016. Voxelizer 3D. URL: https://zmorph3d.com/products/voxelizer-software.